

Use of Streamwise Vorticity to Increase Mass Entrainment in a Cylindrical Ejector

M. J. Carletti* and C. B. Rogers†

Tufts University, Medford, Massachusetts 02155

and

D. E. Parekh‡

McDonnell Douglas Aerospace, St. Louis, Missouri 63166-0516

The following work documents the effect of streamwise vortices generated at the nozzle exit of an axisymmetric air jet on the amount of mass entrained into an ejector. In an experimental analysis of the mass entrainment of circular jet ejectors, we found that the introduction of half-delta-wing vortex generators in the exit of the jet nozzle (Reynolds number of 50,000) increased the amount of entrained mass by as much as 40% over the amount of increase provided by the ejector alone. The effectiveness of the generators was studied for several cases varying ejector diameter, length, spacing, and Reynolds number. Although the performance of an ejector is a strong function of these parameters, the mass entrainment increased in all cases studied due to the presence of the vortex generators.

Nomenclature

| | |
|------------------------------|---|
| A_e | = ejector area |
| A_j | = jet area |
| D_e | = ejector diameter |
| D_j | = jet diameter |
| L_e | = ejector length |
| \dot{m} | = mass flow rate |
| $\dot{m}_{\text{entrained}}$ | = mass entrained into the ejector |
| \dot{m}_{nozzle} | = mass exiting the jet nozzle |
| Re | = Reynolds number, $\bar{U}_{\text{jet}} D_j / \nu$ |
| S | = distance from jet exit to ejector entrance |
| \bar{U} | = time-averaged velocity |
| $\bar{U}_{\text{max}}(0)$ | = centerline velocity at jet exit, $x = 0$ |
| \bar{U}_{plenum} | = average velocity based on jet plenum pressure |
| vor | = vortex case |
| x | = downstream distance from primary jet exit |
| η | = increase in mass entrainment due to vortex generators |
| ν | = kinematic viscosity |
| ρ | = fluid density |

Introduction

OVER the past 40 years, several experimental and analytical studies have been conducted on the thrust augmentation characteristics of jet ejectors. Using the kinetic energy of the primary jet, an ejector causes a pressure drop which induces the flow of a low-energy secondary stream into the ejector. The mixing of the two flows reduces the velocity of the jet within the ejector shroud, while increasing the existing mass flux. By efficiently increasing the mass flow rate through the ejector an increase in thrust can be attained, provided that the resultant decrease in velocity is minimized.

Since the performance of an ejector is dependent on the efficient transfer of momentum between the primary and secondary flows, current research has focused on the improvement of mixing within the ejector shroud. For most aeronautical applications, the mixing of the core flow must occur within a minimum distance so that unnecessary losses due to friction and weight can be avoided. Although

the performance of a larger ejector may be superior, the increase in drag associated with this additional size must be taken into account in terms of practicality and design.

Recent studies have been very successful in enhancing the mixing characteristics of ejectors by introducing vorticity at the exit of the jet nozzle. Using a mixer ejector designed to introduce an array of large-scale, low-intensity streamwise vortices at the exit of a rectangular primary nozzle, Tillman et al.¹ have achieved well-mixed exit flows within two duct diameters.² This design incorporates large-scale streamwise vorticity rather than relying on the shear mixing.¹⁻⁴ It has been shown to be more effective than the previously studied small, intense streamwise vorticity used in hypermixing nozzles that incur large mixing losses.^{5,6} Multiple jet nozzles^{7,8} enhance mixing in ejectors through jet-interaction mechanisms.

The bulk of research on enhancing mixing in jets, however, has focused on free rather than confined jets. Elliptical,⁹ indeterminate origin,¹⁰ and crown nozzle,¹¹ and half-delta-wing vortex generators¹²⁻¹⁴ and tabs^{15,16} have all been shown to increase shear layer growth. Many researchers have also examined active methods including bifurcating and blooming jets^{17,18} and piezoelectric excitation.¹⁹ The current work uses the findings of Surks et al.¹⁴ regarding the effects of streamwise vortices in freejets to improve the performance of circular ejectors.

Although ejector designs have varied greatly in size and aspect ratios, general conclusions can be made for all ejectors. Most of the past literature on ejector designs has shown that the mixing of the inlet streams is the determining factor in the performance of a steady flow ejector. Mixing designs using large-scale, low-loss, streamwise vorticity have been proven to be most effective. Although the mixing within the ejector is most critical, its design must be compact and lightweight in order to be practical. For these reasons this study focuses on increasing the mass entrainment of small, low-aspect-ratio ejectors.

Experimental Apparatus

The experimental study was conducted at the Tufts University Fluids Laboratory. Both centerline velocity and mass entrainment measurements are used to determine the improvement in ejector performance provided by the generators. The mass flux and centerline velocity measurements were obtained on an air jet using a stagnation probe.

Air Jet Facility

Air was supplied to the jet by a compressor, producing a plenum pressure, varying less than 6.5% per run, which was monitored continuously with a pressure port. Each pressure measurement was

Presented as Paper 93-3247 at AIAA Shear Flow Control Conference, Orlando, FL, July 6-9, 1993; received Dec. 13, 1993; revision received Nov. 16, 1994; accepted for publication Dec. 12, 1994. Copyright © 1995 by the American Institute of Aeronautics and Astronautics, Inc. All rights reserved.

*Student, Department of Mechanical Engineering.

†Assistant Professor, Department of Mechanical Engineering. Member AIAA.

‡Principal Technical Specialist. Member AIAA.

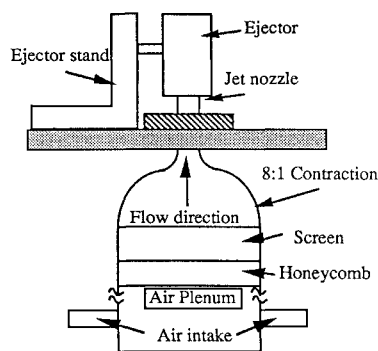


Fig. 1 Tufts air jet facility.

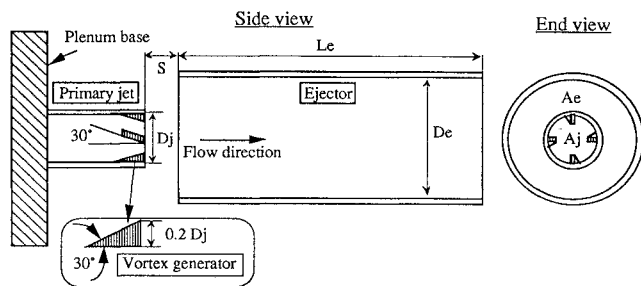


Fig. 2 Ejector setup and parameters.

normalized by the instantaneous plenum pressure to minimize the effect of this drift. The flow enters the plenum through two air intake valves located opposite each other to reduce any swirling effects. The plenum is 28 jet diameters in length, and 8 jet diameters in diameter. Upon entering the plenum the air passes through a honeycomb and then a series of screens. Finally a fifth-order polynomial contraction (64:1 area ratio) reduced the existing diameter to 1.9 cm. Velocities ranging from 7.5 to 30 m/s were used to produce Reynolds numbers from 12,500 to 50,000. Figure 1 presents a schematic of this air jet facility.

Ejector Setup

In order to determine the improvement provided by the half-delta-wing vortex generators, the effects of two primary nozzles were examined for each of the ejectors studied. The first inlet nozzle is an axisymmetric jet, without vortex generators. These cases will be referred to as reference cases. The second inlet nozzle has four half-delta-wing vortex generators, shown in Fig. 2, and will be referred to as the vortex nozzle.

Surks et al.^{13,14} tested many different vortex generator configurations at a Mach number of 0.6 using image analysis and found that the 90-deg symmetric case was the most effective at entraining ambient flow in a relatively high-speed freejet. The vortex nozzle incorporates this 90-deg vortex generator configuration, which is shown in Fig. 2. Using slightly smaller half-delta-wing generators, an increase in mass entrainment of 50% over an axisymmetric jet was produced.

A simple hollow cylinder is used for an ejector in order to isolate the effects of the generators and simplify the analysis. Once the effects of the vortex generators on mass entrainment are better understood, they can be used to further improve many other ejector inlet and outlet designs. Figure 2 shows how vortex generators can be implemented into a basic ejector design model.

The effect of the vortex generators on the performance of circular ejectors was evaluated for many shrouds varying in length L_e , diameter D_e , and spacing S . The parameters varied are shown in Fig. 2. The parameters examined in this study are normalized by the jet diameter D_j and are provided in Table 1. This analysis provided us with information on how the ejector size and position affects the improvement, due to the vortex generators, of ejector performance.

To test the effect of these parameters on ejector performance, each parameter was individually varied while all other characteristics

Table 1 Ejector parameters

| Dimensionless parameters | Lower limits | Upper limits |
|--------------------------|--------------|--------------|
| D_e/D_j | 2 | 4 |
| L_e/D_j | 4 | 12 |
| S/D_j | -2 | 3 |
| Re | 16,667 | 50,000 |

were held at standard dimensions. The standard ejector has a length of 6 jet diameters and a diameter of 2 jet diameters and is positioned flush with the jet exit at spacing of $S = 0$. The baseline Reynolds number is 50,000.

Measurement Techniques and Analysis

A pitot probe was used to acquire the velocity data presented in this study. To calculate the increase in mass entrainment produced by the ejector, pressure measurements were taken in a two-dimensional grid at both the exit of the jet nozzle (in the absence of the ejector) and the ejector exit. One of the limitations of this work is that we assume no change in the exit conditions of the primary nozzle due to the presence of the ejector shroud. A two-dimensional computer-controlled traversing mechanism was used to position the probe within ± 0.0125 mm of the desired location. The velocity at each point in the profile was determined from an average of 1000 pressure samples taken over 1.5 s. Each point was normalized by a simultaneous plenum pressure measurement.

To quantify the effectiveness of an ejector as a pumping mechanism, we have focused on the ejector's ability to entrain mass and, thus, increase pumping efficiency. This improvement is defined as the difference in mass entrainment between the vortex and reference cases normalized by the amount of mass entrained in the reference case

$$\eta = \frac{[\dot{m}_{\text{entrained}}/\dot{m}_{\text{nozzle}}]_{\text{vor}}}{[\dot{m}_{\text{entrained}}/\dot{m}_{\text{nozzle}}]_{\text{ref}}} - 1 \quad (1)$$

The mass entrainment fraction, calculated in Eq. (1), is derived from simple mass flow analysis described in Ref. 20.

All measurements of mass entrainment are normalized by the individual mass flux of the particular nozzle tested. The projected area of the jet nozzle varies significantly between the reference and vortex cases. Because of the blockage created by the generators, the vortex nozzle has an effectively smaller area; thus, its mass flux will correspondingly be lower. The effective blockage of the vortex generators is approximately 11% of the nozzle's exit area.

In a comparison of several identical runs, done on different days, the repeatability of the centerline data is within 2%. The repeatability of the centerline profiles within the first 6 jet diameters downstream of the jet exit, however, is within 0.5%. Each velocity measurement is assumed to have a maximum error of 2%. Since the normalized mass entrainments in Eq. (1) are a function of multiple velocity readings, they have a maximum error of 8%.

Centerline Velocity Decay

The figures presented in this section show the decay of the geometric centerline velocity from the primary nozzle exit. The data presented show the percent decrease in centerline velocity due to the vortex generators. The use of the contour plots in Figs. 5–7 allows for a clear and concise presentation of data which would be otherwise difficult to read if presented on standard centerline graphs.

Jet Flow—Centerlines Profiles

The centerline velocity of a standard axisymmetric jet, without an ejector, begins decaying at approximately 4 jet diameters downstream of the nozzle. Inserting the vortex generators, in the 90-deg symmetric configuration, causes the decay of the centerline to occur much sooner, at approximately 2.5 jet diameters. The centerline velocity is unaffected by the generators upstream of this point (see Fig. 3). The symmetric vortex configuration chosen produces large-scale, corotating vortex structures that inviscidly stir the flow to

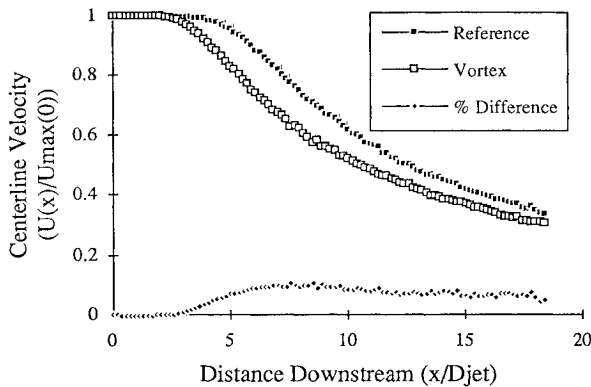


Fig. 3 Effect of vortex generators on centerline decay without an ejector.

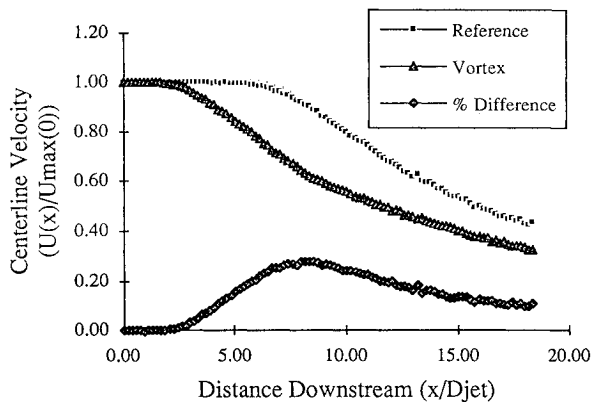


Fig. 4 Effect of vortex generators on centerline decay for standard ejector.

increase mixing. The decay of the centerline velocity is a good relative measure of increased mixing for the symmetric configurations over an axisymmetric jet, since the core is not vectored off of the jet's centerline axis, as is observed in counter-rotating vortex generation methods.

Ejector Flow—Centerlines Profiles

A comparison of the centerline velocity decay through a standard ejector for the reference and vortex cases is shown in Fig. 4. This graph is in the conventional style for centerline plots. The vertical axis shows the centerline velocity of the jet flow at any position downstream normalized by the centerline velocity at the jet exit. The horizontal axis represents the distance downstream of the jet nozzle normalized by jet diameter. As in Fig. 3, the no-ejector case, the decay of the centerline with the vortex nozzle occurs noticeably sooner than for the reference nozzle. The centerline decay of the reference jet issuing into a standard ejector is similar in shape to that of the unshrouded jet shown in Fig. 3. The ejector shroud, however, delays the onset of decay by an additional distance of 1.5 jet diameters downstream. By preventing the spread of the shear layer, the ejector acts as a shield inhibiting the potential core from mixing with the ambient fluid and delaying any significant centerline velocity decay until beyond the ejectors exit. In the case of the vortex nozzle with a standard ejector, the core velocity begins to decay at the same location as the enshrouded nozzle at 2.5 jet diameters downstream. The large-scale mixing due to the vortex generators is evident even though the spreading of the shear layer is impeded by the ejector walls. At the ejector exit the centerline velocity of the vortex case has decreased 23% as compared to 1% for the reference nozzle due to the increased mixing resulting from the additional streamwise vorticity introduced by the generators.

In an effort to simplify the presentation of the centerline data for parameter variation, contour plots showing the percent difference between the centerline decay of the reference and vortex cases will be used. The distance downstream of the jet exit is shown on the vertical axis, and the ejector parameter (e.g., diameter, length, or

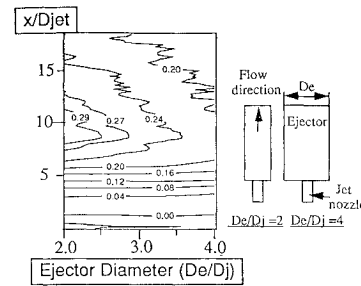


Fig. 5 Percent decrease in centerline velocity due to vortex nozzle with diameter variation.

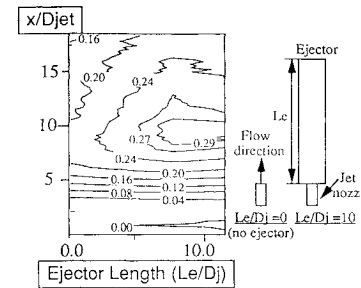


Fig. 6 Percent decrease in centerline velocity due to vortex nozzle with length variation.

spacing) being varied is shown on the horizontal axis. The contour levels show the percent difference between the centerline velocity of the vortex and reference ejectors.

In the variation of ejector diameter, all other parameters are held constant. All of the ejectors have a standard length of 6 jet diameters, and are at a standard spacing of zero (the ejector entrance is flush with the jet nozzle exit). The effect of varying ejector diameter on the velocity decay of the potential core is illustrated in Fig. 5. Ejector diameter, shown on the x axis, is varied between 2 and 4 jet diameters. The plot shows a linear interpolation between the diameters studied (2.0, 2.67, 3.33, 4.0). Within 2.5 jet diameters of the jet exit there is essentially no difference between the two cases. Inside the ejector shroud, up to 6 jet diameters downstream of the jet nozzle, the percent decrease in centerline velocity due to the vortex generators is independent of ejector diameter. In fact, the centerline decay for the vortex nozzle is essentially independent of ejector diameter. This again shows that the decay of the centerline is predominantly a result of the vortex mixing rather than shear layer spreading. The change in percent difference comes from the effect of diameter variation on the decay of the reference nozzle. Beyond the ejector exit the percent decrease in centerline velocity is much more significant for smaller diameter ejectors. This is because the smaller diameter ejectors allow less spreading of the shear layer in the reference cases.

Adjusting the length of the ejector, with diameter held at a standard of 2 jet diameters and a standard spacing of zero, has very little effect on the centerline velocity decay of either the reference or vortex cases within the first 5 jet diameters downstream. This is illustrated in Fig. 6, which shows the difference in centerline decay for a variation of ejector length from 0 to 12 jet diameters (equivalent to 0–6 ejector diameters). Only a slight deviation is shown for the no-ejector case ($L = 0$) which is due to the reference case decaying more rapidly due to the absence of the ejector shroud. Beyond 6 jet diameters downstream, the vortex-generators have the greatest impact on the decay of the centerline velocity for ejector lengths between 4 and 8 jet diameters.

Centerline velocity decay for the reference case is delayed until the ejector's exit up to an ejector length of approximately 8 jet diameters, beyond which the decay begins within the ejector shroud. The decay of the centerline for the vortex nozzle begins within the ejector shroud, at approximately 2.5 jet diameters downstream of the jet exit, regardless of the length of the ejector, for the cases studied.

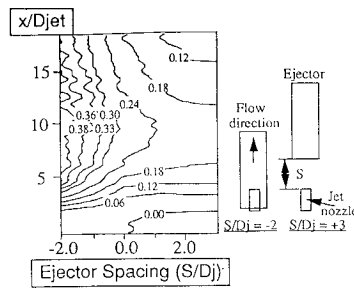


Fig. 7 Percent decrease in centerline velocity due to vortex nozzle with spacing variation.

Figure 7 is a contour plot illustrating the effect of varying ejector spacing on the percent decrease in centerline velocity of the vortex nozzle over the reference nozzle. The variation of position from $S/D_j = -2$ to $S/D_j = +3$ of a standard ejector ($L/D_j = 6$ and $D/D_j = 2$) is shown on the horizontal axis. The decrease in centerline velocity is highly dependent on the downstream location of the ejector. The impact of the vortex generators increases as the ejector shroud is positioned farther upstream. It is important to point out that at an ejector spacing of $S/D_j = -2$, the ejector shroud is within 3 mm of the plenum base, severely limiting the mass entrainment in both the reference and vortex nozzle cases.

Finally, we found that the velocity decay of the centerline for the vortex ejector is essentially independent of Reynolds number from 15,000 to 50,000. Once the jet becomes turbulent, the centerline decay through the ejector is not significantly dependent on the Reynolds number. For lower Reynolds numbers the decay of the centerline occurs slightly faster. Again, the reference nozzle seems to be more affected by the variation than does the vortex case. The streamwise vorticity introduced to the flow stirs the ambient, low-speed, fluid into the potential core. This causes a much more rapid deterioration than the viscous spreading of the shear layer.

Although the decay of the centerline velocity is not the best indicator of ejector efficiency, it has provided insight into the effect of the vortex generators on the increase in mixing within the ejector shroud. The centerline decay of the vortex nozzle is independent of the presence of the shroud. The rapid decay of the centerline velocity due to the generators implies that the flow existing the ejector shroud is better mixed than in the reference case. Again, this is a more valid inference for symmetric cases than for asymmetric configurations which vector the core flow off of centerline resulting in a dramatic decrease in centerline velocity. By increasing the rate of mixing within the ejector shroud the pumping efficiency of the ejector improves.

Mass Entrainment Measurements

Two-dimensional profiles taken at the exit of the reference and vortex primary nozzles (in the absence of an ejector shroud) are shown in Fig. 8. For all two-dimensional profiles, the measurement grid step size is 0.127 cm. Figure 9 presents a comparison between normalized velocity profiles of the reference and vortex nozzles at the ejector's exit. These profiles were taken at the exit of the standard ejector for each of the two cases. Each point on the following graphs (Figs. 10–12) is derived from the analysis of similar plots. This figure illustrates the distinct flow pattern generated by the vortex nozzle. The ejector on the left, the reference case, shows little spreading of the potential core. The center of the ejector has a velocity of nearly equal to that at the jet exit, and little mixing has occurred, since the velocity at the edge of the ejector is essentially zero. In the vortex nozzle, on the right, the dark region representing the potential core is spread out by the vorticity introduced by the generators. Although there is no region of velocity equal to that exiting the primary jet nozzle, the mixing enhancement due to the generators has provided a more uniform velocity profile at the ejector exit. As a result of the streamwise vorticity, the velocity map of the vortex ejector exit is similar in shape to the vortex nozzle exit profile shown in Fig. 8.

Through the acquisition of two-dimensional exit velocity profiles of both the jet nozzle and the ejector, the amount of mass entrained can be determined using Eq. (1). Figures 10–12 show the mass

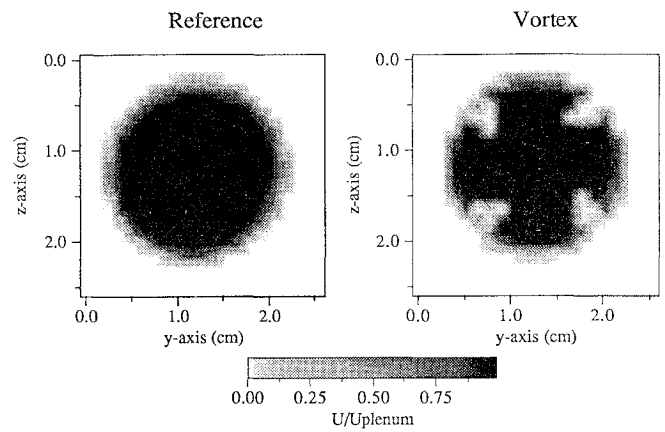


Fig. 8 Effect of vortex generators on the exit velocity profile of the primary nozzle.

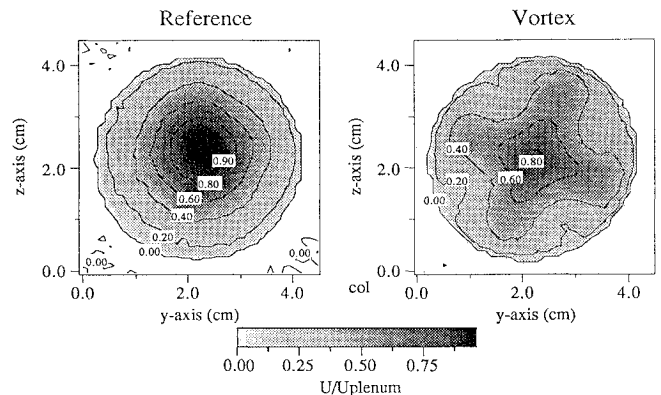


Fig. 9 Effect of vortex generators on the exit velocity profile of the standard ejector.

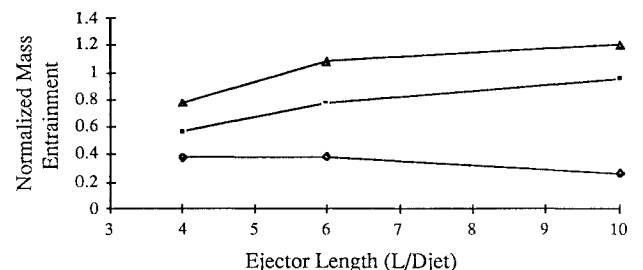


Fig. 10 Effect of ejector length on the mass entrainment for the reference and vortex cases: —■— reference, —◆— vortex, —▲— mass entrainment fraction.

entrainment of both the reference and vortex ejectors normalized by the corresponding primary nozzle, as well as the mass entrainment fraction η , showing the increase in mass entrainment for each of the ejectors due to the half-delta-wing vortex generators.

The increase in mass entrainment with the vortex nozzle indicates that the half-delta-wing vortex generators improve the effectiveness of the ejector at entraining fluid. Figure 10 presents the normalized mass entrainment of each nozzle, as well as the increase in mass entrainment of the vortex case over the reference case, as a function of ejector length. The shroud length is varied from 4 to 10 jet diameters. There is an increase in mass entrainment for both nozzles as the ejector shroud is lengthened. This increase becomes more gradual as the ejector length approaches 10 jet diameters. However, in many applications a longer ejector is inefficient due to increased drag.

The improvements due to the vortex generators are greater for shorter length ejectors. Further, for shorter length ejectors, the increase in mass entrainment due to the generators is approximately 40%. Beyond an ejector length of 6 jet diameters, there is a decrease in the mixing benefits of the generators with increase in ejector

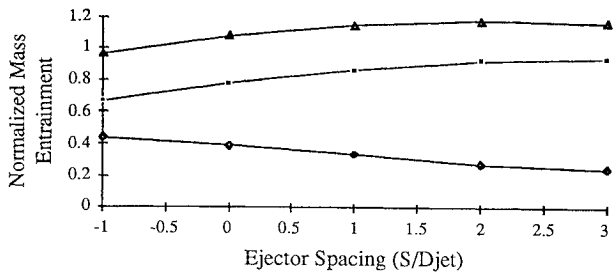


Fig. 11 Effect of ejector spacing on the mass entrainment for the reference and vortex cases: —■— reference, —◆— vortex, —▲— mass entrainment fraction.

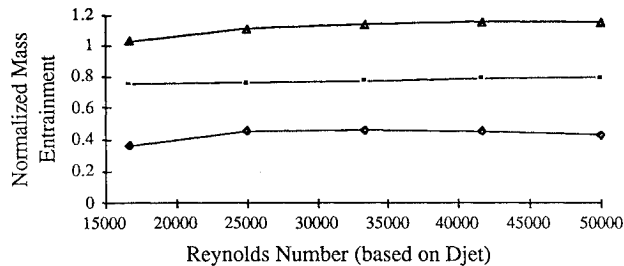


Fig. 12 Effect of Reynolds number on the mass entrainment for the reference and vortex cases: —■— reference, —◆— vortex, —▲— mass entrainment fraction.

length. This again shows that most of the mixing improvement due to the generators occurs near the jet exit.

As the ejector is moved farther downstream, it becomes more efficient at entraining mass, however, the percent improvement due to the generators decreases. This decrease in percent improvement is illustrated in Fig. 11. The vortex nozzle is most effective for the negative spacings, due to the shorter mixing region. The percent improvement decreases with an increase in spacing. This trend is comparable to the data presented for length variations in Fig. 10.

The effects of ejector spacing can be correlated using an ejector mixing length, defined as the distance from the exit of the jet nozzle to the exit of the ejector. For example, for an ejector length of 6 jet diameters, the mixing length for $S/D_j = -1$ is 5 jet diameters, and the mixing length for $S/D_j = +3$ is 9 jet diameters. When these data are compared to standard ejector data for $S/D_j = 0$ and $L/D_j = 5$ and 9, the data correspond to within 5%. This shows that the entrainment characteristics of an ejector are well correlated with the length of the mixing region.

Figure 12 shows the change in mass entrainment for both the reference and vortex cases with a variation in Reynolds number. Within a variation of Reynolds number from 17,000 to 50,000, the reference case shows no difference in the amount of entrained mass. The vortex case, on the other hand, shows a slight increase in the amount of entrained mass with an increase in Reynolds number. This variation in mass entrainment, however, is much less than when the ejector's physical parameters are varied.

Conclusions

The addition of large-scale streamwise vortices at the nozzle exit increases centerline velocity decay, mass entrainment, and shear layer spreading within a simple circular ejector. The 90-deg symmetric configuration of half-delta-wing vortex generators used in this study produces a set of four corotating vortices that enhance mixing within the ejector. The initial centerline velocity decay in the vortex case is only weakly dependent on ejector parameters, implying that the streamwise vorticity dominates within the first five diameters of the nozzle exit.

The results presented on the mass entrainment of the vortex ejector show more than a 40% increase in mass entrainment due to the

presence of the vortices. Although the vortex cases always showed an improvement over the reference cases, the most attractive feature of the generators is that they show the greatest improvement for the more compact ejector configurations. Thus, the use of vortex generators would be especially beneficial for smaller and shorter ejectors which are typically preferred for practical considerations. This study, to date, has only examined the increase in mass entrainment into a simple cylindrical ejector shroud. A more sophisticated ejector with a contoured entrance and diffusing exit would be needed to produce a significant increase in thrust.

Acknowledgments

This research was conducted under the joint sponsorship of the McDonnell Douglas Corporation and Tufts University. The authors are grateful to Vincent Miraglia and James Hoffman for their assistance in the design and construction of the experimental apparatus.

References

- ¹Tillman, T. G., Peterson, R. W., and Presz, W. M. J., "Supersonic Nozzle Mixer Ejector," *Journal of Propulsion and Power*, Vol. 8, No. 2, 1992, pp. 513–519.
- ²Presz, W. M. J., and Greitzer, E. M., "A Useful Similarity Principle for Jet-Engine Exhaust System Performance," AIAA Paper 88-3001, July 1988.
- ³Presz, W. M. J., Morin, B. L., and Gousy, R. G., "Forced Mixer Lobes in Ejector Designs," *Journal of Propulsion and Power*, Vol. 4, No. 4, 1988, pp. 350–355; also AIAA Paper 86-1614, June 1986.
- ⁴Skebe, S. A., McCormick, D. C., and Presz, W. M. J., Jr., "Parameter Effects on Mixer-Ejector Pumping Performance," AIAA Paper 88-0188, Jan. 1988.
- ⁵Bevilaqua, P. M., "Evaluation of Hypermixing for Thrust Augmenting Ejectors," *Journal of Aircraft*, Vol. 11, No. 6, 1974, pp. 348–353.
- ⁶Bevilaqua, P. M., and McCullough, J. K., "Entrainment Method for V/Stol Ejector Analysis," AIAA 9th Fluid and Plasma Dynamics Conference, San Diego, CA, July 1976.
- ⁷Chandrasekhara, M. S., Krothapalli, A., and Baganoff, D., "Mixing Characteristics of a Supersonic Multiple Jet Ejector," AIAA Paper 87-0248, Jan. 1987.
- ⁸Chandrasekhara, M. S., Krothapalli, A., and Baganoff, D., "Performance Characteristics of an Underexpanded Multiple Jet Ejector," *Journal of Propulsion and Power*, Vol. 7, No. 3, 1990, pp. 462–464.
- ⁹Ho, C.-M., and Gutmark, E., "Vortex Induction and Mass Entrainment in a Small-Aspect, Ratio Elliptic Jet," *Journal of Fluid Mechanics*, Vol. 179, June 1987, pp. 383–405.
- ¹⁰Wlezien, R. W., and Kibens, V., "Passive Control of Jets with Indeterminate Origins," *AIAA Journal*, Vol. 24, No. 8, 1986, pp. 1263–1270.
- ¹¹Longmire, E. K., Eaton, J. K., and Elkins, C. J., "Control of Jet Structures by Crown-Shaped Nozzle Attachments," AIAA Paper 91-0316, Jan. 1991.
- ¹²Rogers, C. B., and Parekh, D. E., "Mixing Enhancement by and Noise Characteristics of Streamwise Vortices in an Air Jet," *AIAA Journal*, Vol. 32, No. 3, 1994, pp. 464–471.
- ¹³Surks, P., Rogers, C. B., and Parekh, D. E., "Entrainment and Acoustic Variations in a Round Jet from Introduced Streamwise Vorticity," *AIAA Journal*, Vol. 32, No. 10, 1994, p. 2108.
- ¹⁴Surks, P., Rogers, C. B., and Parekh, D. E., "The Effect of Streamwise Vorticity on the Mixing and Acoustic Characteristics of an Axisymmetric Jet," Tufts Univ., TR-TF-892, Medford, MA, Aug. 1992.
- ¹⁵Samimy, M., Reeder, M., and Zaman, K., "Supersonic Jet Mixing Enhancement by Vortex Generators," AIAA Paper 91-2263, June 1991.
- ¹⁶Zaman, K. B. M. Q., Samimy, M., and Reeder, M. F., "Effect of Tabs on the Evolution of an Axisymmetric Jet," *Eighth Symposium on Turbulent Shear Flows* (Technical Univ. of Munich), 1991, pp. 25-5-1–25-5-6.
- ¹⁷Lee, M., and Reynolds, W. C., "Bifurcating and Blooming Jets," 5th Symposium on Turbulent Shear Flows, Ithaca, NY, Aug. 1985.
- ¹⁸Parekh, D. E., Reynolds, W. C., and Mungal, M. G., "Bifurcation of a Round Air Jet by Dual Mode Acoustic Excitation," AIAA Paper 87-0164, Jan. 1987.
- ¹⁹Wiltse, J. M., and Glezer, A., "Manipulation of Free Shear Flows Using Piezoelectric Actuators," *Journal of Fluid Mechanics*, Vol. 249, April 1993, pp. 261–285.
- ²⁰Carletti, M. J., Rogers, C. B., and Parekh, D. E., "The Use of Streamwise Vorticity to Enhance Ejector Performance," Tufts Univ., TR-TF-893, Medford, MA, Aug. 1993; also AIAA Paper 93-3247, July 1993.